TNFα/Grnd mediate JNK/MMPs activation during glioma progression and neurodegeneration

Marta Portela[1,2,#,*], Teresa Mitchell[1,#] and Sergio Casas-Tintó[1,*]

1-Instituto Cajal-CSIC. Av. del Doctor Arce, 37. 28002. Madrid. Spain

2-Current address: Department of Biochemistry and Genetics, La Trobe Institute for Molecular Sciences, LaTrobe University, Melbourne, Australia

[#]Co-first authors

*Corresponding authors: m.portelaesteban@latrobe.edu.au

scasas@cajal.csic.es

Summary

Glioblastoma (GB) is a type of brain tumour that involves the transformation of glial cells. This is the most aggressive and lethal tumour of the central nervous system and currently there are not efficient treatments. In GB, glial cells display a network of membrane projections (cytonemes) which mediate cell to cell communication. Under pathological conditions like GB, cytonemes transform into ultra-long tumour microtubes (TMs) that infiltrate into the brain, enwrap neurons and deplete wingless (Wg)/WNT from the neighbouring healthy tissue. GB cells establish a positive feedback loop including Wg signalling, JNK and matrix metalloproteases (MMP) required for GB progression and neuronal synapse loss and degeneration. Frizzled1 receptor mediates Wg signalling upregulation which is required for JNK activation in GB. Consequently, MMPs are upregulated and facilitate TMs infiltration in the brain, hence GB TMs network expands and mediate further Wg depletion to close the loop. Thus, cellular signals other than primary mutations emerge as a central feature of GB which correlates with a poor prognosis in patients and animal models. Here we describe the molecular mechanisms that regulate TMs production, infiltration and maintenance, in a *Drosophila* model of GB. The contribution of the bi-directional signals between healthy tissue (neurons) and GB cells, mediate the

progression of the disease. JNK pathway signalling mediated by Grindelwald (Grnd) receptor is activated by the ligand Eiger (Egr)/TNFα secreted by the neurons surrounding the GB. Then, MMPs are secreted to facilitate TM progression and GB dissemination. Here we show that the coordination among different signals facilitate GB progression and contribute to the complexity and versatility of these incurable tumours.

Keywords

Glia, Cancer, Glioblastoma, Tumour Microtubes, JNK, Neurodegeneration.

Introduction

Glioblastoma multiforme (GB) is the most frequent and aggressive primary malignant brain tumour with a 3 per 100.000 incidence per year (Gallego 2015). GB patients´ median survival is 12-15 months, with less than 5% of survival after 5 years (Gallego 2015; McGuire 2016; Rogers *et al.* 2018; Louis *et al.* 2016). The causes of GB are under debate (McGuire 2016), 5% of the patients develop GB after a low grade astrocytoma (Alifieris & Trafalis 2015) and the most frequent mutations include gain of function of the epidermal growth factor receptor (EGFR) (97%) and the phosphatidylinositol-3 kinase (PI3K)/ phosphatase and tensin homologue (PTEN) pathways (88%) (Hayden 2010). The diagnosis, and therefore the treatment of GB, requires a mutation analysis taking into account the high frequency of clones within the same primary GB (Wick *et al.* 2018). Temozolomide (TMZ) has emerged as an effective treatment for GB however, recent discoveries restrict the use of TMZ in GB patients depending on the methylation status of *methylguanine DNA methyltransferase (MGMT) (Wick et al. 2018)*. Moreover, among other mutations, *Isocitrate dehydrogenase (IDH)* define the nature and features of GB (Waitkus *et al.* 2018) together with molecular alterations including 1p/10q deletions and *tumour suppressor protein 53 (TP53)* and *alpha thalassemia/mental retardation (ATRX)* mutations (Waitkus *et al.* 2018;

Miller *et al.* 2017). This genetic and molecular heterogeneity difficult the diagnosis and treatment of this fatal brain tumours.

The recent discovery of a network of ultra-long tumour microtubes (TMs) in GB (Osswald *et al.* 2015) improves our understanding of GB progression and therapy resistance (Osswald *et al.* 2016). TMs are actin-based filopodia which infiltrate into the brain and reach long distances within the brain (Osswald *et al.* 2015). TMs are required in GB cells to mediate Wingless (Wg)/WNT signalling imbalance among neurons and GB cells. Wg/WNT signal is favoured in GB cells to promote proliferation, at expenses of the neurons which undergo degeneration and cause lethality (Arnes & Casas Tinto 2017; Portela *et al.* 2019; Casas-Tinto & Portela 2019). The central role of TMs in GB biology has emerged as a fundamental mechanism for GB rapid and lethal progression thus; it is an attractive field of study towards potential GB treatments. However, the molecular mechanisms underlying the expansion of TMs are not well understood and the signalling pathways mediating TM infiltration are still unknown.

The Jun-N-terminal Kinase (JNK) pathway has been associated to glial proliferation. GB cells normally activate JNK pathway to maintain the stem-like GB cells, which has become a pharmacological target for the treatment of GB (Matsuda *et al.* 2012). Moreover, the JNK pathway is the main regulator of Matrix metalloproteases (MMPs) expression and cell motility in different organisms and tissues (Zeigler *et al.* 1999; Lee *et al.* 2009; Uhlirova & Bohmann 2006; Cheng *et al.* 2012; Ispanovic & Haas 2006).

MMPs are a family of endopeptidases capable of degrading the extracellular matrix (ECM). Members of the MMP family include the "classical" MMPs, the membrane-bound MMPs (MT-MMPs), the ADAMs (a disintegrin and metalloproteinase; adamlysins) and the ADAMTS (a disintegrin and metalloproteinase with thrombospondin motif). There are more than 20 members in the MMP and ADAMTS family including the collagenases, gelatinases, stromelysins, some elastases and aggrecanases (Malemud 2006). The vertebrate MMPs

have genetic redundancy and compensation, they have overlapping substrates, and pharmacological inhibitors are non-specific. There are two orthologues to human MMPs in *Drosophila*, *MMP1* and *MMP2*. MMP1 is secreted and MMP2 is membrane-anchored. However, recent reports propose that products of both genes are found at the cell surface and released into media, and that GPI-anchored MMPs promote cell adhesion when they become inactive. Moreover, the two MMPs cleave different substrates, suggesting that this is the important distinction within this small MMP family (LaFever *et al.* 2017). MMPs are upregulated in several tumours, including gliomas. Cancer cells produce MMPs to facilitate tumour progression and invasiveness and MMPs upregulation in GB is associated with the diffuse infiltrative growth and have been proposed to play a role in glioma cell migration and infiltration (Veeravalli & Rao 2012; de Lucas *et al.* 2016) reviewed in (Nakada *et al.* 2003). MMPs are upregulated in human GB cell-lines and biopsies as compared with low-grade astrocytoma (LGA) and normal brain samples (Hagemann *et al.* 2012; Hagemann *et al.* 2010). In particular, among the 23 MMPs present in humans, MMP9, MMP2 and MMP14 are directly implicated in growth and invasion of GB cells (Munaut *et al.* 2003).

WNT induces MMPs expression during development and cancer (Lyu & Joo 2005; Uraguchi *et al.* 2004; Lowy *et al.* 2006; Roomi *et al.* 2017; Page-McCaw *et al.* 2003) associated to cell migration and metastasis. Specifically, in human GBs, MMP2 expression and their infiltrative properties correlate with Wnt5 (Kamino *et al.* 2011; Roth *et al.* 2000) and MMP9 is upregulated upon EGFR activity (Chen *et al.* 2016).

In consequence, MMPs upregulation in GB is an indicator of poor prognosis (Yamamoto *et al.* 2002) and the study of the mechanisms mediated by MMPs is relevant for the biology of GB, and cancer in general. GB cells project TMs which cross the extracellular matrix (ECM) and break in the brain to reach territories distant from the original GB site (Osswald *et al.* 2015; Osswald *et al.* 2016).

We have previously demonstrated that GB cells activate the JNK pathway and accumulate MMPs (MMP1 and 2). MMPs contribute to TMs expansion through the brain and facilitate Frizzled1-mediated Wg/WNT signalling in GB cells. Moreover, Wg/WNT signalling mediates JNK activation in GB cells to continue with the process. We hypothesize that the founder mutations in GB (PI3K and EGFR) initiate the process with the expansion of the TMs; afterwards, the system self-perpetuates (TMs-Fz1/Wg-JNK-MMPs-TMs) to facilitate GB progression and infiltration in the brain (Portela *et al.* 2019).

JNK pathway depends on the formation of the TMs network as well as the presence of Fz1 receptor in GB cells. JNK signalling pathway is required for normal glial development and GB progression and proliferation. However, JNK pathway activation mediated by the receptor grnd is a requirement for TMs formation, and Fz1 re-localization in the areas of contact with neurons that mediate neuronal Wg depletion. Fz1 accumulation in GB leads to activation of the Wg pathway that in turn, induce JNK activity in GB cells. JNK pathway activation mediate the production of matrix metalloproteinases (MMPs) to facilitate ECM digestion that allows TMs infiltration and invasion into the brain that results in premature death (Portela *et al.* 2019).

MMPs mediate GB progression, but also mediate neurodegeneration. *MMPs* silencing in GB cells is sufficient to rescue synapse loss in the neighbouring neurons and to rescue the life span in adult flies. These results bring a novel positive feedback loop including Wg pathway, JNK and MMPs which contribute to GB development (Portela *et al.* 2019), thus opening novel avenues for GB adaptation mechanisms and potential pharmacological targets.

Here we describe the molecular mechanisms behind TMs production, infiltration and maintenance in a *Drosophila* GB model. The contribution of the bi-directional signals between healthy tissue (neurons) and GB cells, mediate the progression of the disease (Portela *et al.* 2019; Jarabo *et al.* 2020). JNK pathway signalling mediated by Grnd receptor is activated by Egr secreted by the neurons surrounding the GB. Then, MMPs are secreted

to facilitate TM progression and GB dissemination. Here we show that the coordination among different signals facilitate GB progression and contribute to the complexity and versatility of these incurable tumours.

RESULTS

PI3K or EGFR individually are not sufficient to stimulate MMPs expression

The most common causes of GB include gain of function mutations in EGFR and PI3K/PTEN pathways. The *Drosophila* GB model reproduces the main features of the disease including the development of a glioma network. To decode the signals responsible for the growth of the TM network, we analyzed EGFR and PI3K/PTEN pathways independently. First, we analyzed Fz1 localization in the brain which is key to trigger Wg signaling and glial proliferation. We assessed the presence of Fz1 receptor in glial membranes. A specific monoclonal antibody was used to visualize the Fz1 receptors that are localized homogeneously across the brain in control samples (Figure S1A). However, in the GB model, the TMs expand and accumulate Fz1 (Figure S1B). To determine if expression of constitutively active forms of PI3K or EGFR alone is sufficient to trigger TMs network expansion and Fz1 accumulation, we expressed *Drosophila PI3K* or *EGFR* (*UAS-dp110^{CAAX} or UAS-TOR-DER^{CA}*) in glial cells under *Repo-Gal4* regulation and stained with Fz1 antibody. The results show that Fz1 receptors localized homogeneously across the brain (Figure S1C-D) similar to control samples, and the glial TM network does not expand (compare Figure S1C-D to Figure S1A-B). These data suggest that the activation of both pathways together is necessary for the expansion of the TMs network and Fz1 accumulation.

PI3K and EGFR pathways converge in *dMyc* expression and *dMyc* is required for GB development (Read *et al.* 2009; Wang *et al.* 2017; Annibali *et al.* 2014; Tateishi *et al.* 2016). Thus, to determine if d*Myc* is sufficient to trigger TMs network and Fz1 accumulation, we

expressed d*Myc* (*UAS-dMyc*) in glial cells under *Repo-Gal4* regulation and stained the brains with Fz1 (Figure S1E), Wg (Figure S1F-H) and Cyt-Arm antibodies (Figure S1I-K). The confocal images do not show morphological evidence of glioma and the TMs glial network does not expand (Figure S1E compare to glioma in S1B). Moreover, no detectable Wg or Fz1 proteins were found in the glial membranes (Figure S1E-H) and Cyt-Arm is homogeneously distributed along the brain (Figure S1K compare to glioma in S1J) similar to control samples (Figure S1I). Taking these results together, *dMyc* it is not sufficient to reproduce the features of the GB even though it is a convergent point of EGFR and PI3K pathways. These results suggest that both PI3K and EGFR together are necessary to activate a pathway downstream responsible for the expansion of glial projections, Fz1 accumulation and activation of the Wg pathway in glial transformed cells, and dMyc signaling is not sufficient to cause these phenotypes.

To determine the epistatic relations behind MMPs expression, we studied single gene modifications related to GB and the effect on MMPs. We analyzed MMP1 localization in the brain which is key to trigger TMs expansion and is a target of the JNK pathway. We assessed the presence of MMP1 in glial membranes. A specific monoclonal antibody was used to visualize the MMP1 that localized homogeneously across the brain in control samples (Figure 1A). However, in the GB brain, the TMs expand and accumulate MMP1 (Figure 1B). Again, we expressed separately the constitutively active forms of PI3K (*dp110*^{CAAX}) and EGFR (*TOR-DER*^{CA}) in glial cells marked with ihog-RFP. In both cases we did not observe a significant upregulation of MMP1 or the formation of TMs (Figure 1C-D, quantified in F). Besides, we also tested *dMyc* upregulation in glial cells as a candidate to upregulate MMP1. However, we did not observe any significant change in MMPs expression or localization upon *dMyc* upregulation (Figure 1E-F). Taking these results together, EGFR, PI3K or dMyc are not sufficient to reproduce the features of glioma. These results suggest that the combined activity of PI3K and EGFR pathways are necessary to activate a downstream pathway responsible for the expansion of TM glial projections and MMP1

accumulation in glial transformed cells, but *dMyc* expression is not sufficient to cause these phenotypes.

Egr/Grnd in GB

A recent study using gene expression profiling identified genes that were significantly correlated with the overall survival in patients with GB and were further analysed for their involvement in pathways and possible biological roles. Eight pathways were identified as core pathways. Half of these pathways were signal transduction pathways correlated with cell survival, death, and growth. 104 genes were identified, which are common between patients with GB and those with low grade gliomas and can be used as core genes related to patient survival. Of these, 10 genes (CTSZ, EFEMP2, ITGA5, KDELR2, MDK, MICALL2, MAP 2 K3, PLAUR, SERPINE1, and SOCS3) can potentially classify patients with gliomas into different risk groups and could be used to estimate the prognosis of patients with gliomas. Among these pathways identified from the enrichment analysis of survival-related genes, the TNF-alpha signalling pathway stands out. Four genes from this 10-gene group (MAP 2 K3, PLAUR, SERPINE1, and SOCS3) are involved in TNFα signalling, and they might have potential prognostic value for patients with GB, (Hsu *et al.* 2019).

Moreover, the expression profiles of these potential biomarkers could be correlated to the molecular subtypes of patients, such as IDH1/2 mutation/wild type and chromosome 1p/19q codeletion/noncodeletion (Hsu *et al.* 2019).

Due to the relevance of TNFα signalling in GB we decided to study Egr, that is the solely *Drosophila* orthologue of the ligand for the mammalian Tumour Necrosis Factor (TNF)-TNF Receptor signalling pathway (Igaki *et al.* 2002; Moreno *et al.* 2002), in the *Drosophila* GB model.

Egr translocates from Neuron to Glia in GB and Grnd accumulates in GB cells

The *Drosophila* orthologue of TNFα and its receptor are Egr and grnd respectively. We used an *Egr-GFP* protein fusion and monitored GFP signal in the *Drosophila* brain. The results from confocal microscopy show that most Egr-GFP signal is localized in the neurons (~70%) that contact with glial cells in control brains (Figure A-B, E). However, there is a shift of Egr-GFP signal from neurons to glia (~50%) in GB samples (Figure 2C-E). Next, we monitored the expression pattern of the JNK receptor grnd, with a specific antibody in GB and control samples (Figure 2F-H). The results show that grnd protein accumulates in GB brains. Taking these data together, GB cells accumulate grnd and Egr protein translocates from neurons to glia in GB brains. Thus, we propose that Egr produced in neurons mediates JNK pathway activation in GB cells.

Progressive JNK activation in glioma

JNK is upregulated in a number of tumours including GB and it is related to glioma malignancy (Hagemann *et al.* 2005; Zeng *et al.* 2018; Mu *et al.* 2018; Huang *et al.* 2003). Moreover, JNK is a target for specific drugs in combination with temozolomide treatments as it was proven to play a central role in GB progression (Matsuda *et al.* 2012; Kitanaka *et al.* 2013; Feng *et al.* 2016; Okada *et al.* 2014). However, little is known about the molecular mechanisms underlying JNK activation in glioma cells and the functional consequences for GB progression.

We had previously confirmed JNK pathway activation in GB cells, by using the *TRE-RFP* reporter that confer transcriptional activation in response to JNK signalling (Chatterjee & Bohmann 2012; Jemc *et al.* 2012; Ruan *et al.* 2016). Now we decided to study the activation of the JNK pathway in a timely manner to understand when is the JNK activated in GB. We took advantage of another JNK reporter (*puc-LacZ*) that monitors the transcriptional activation of the downstream JNK target *puckered (Martin-Blanco et al. 1998; Langen et al.*

2013). To analyse JNK activity in GB at two different timepoints (48 and 96h after GB induction), we used the thermo sensitive repression system Gal80TS that restricts the expression of the GAL4/UAS system (see materials and methods). In control brains, the JNK reporter *puc-LacZ* is mostly activated in neurons (~78%). 48h after the induction of the GB, *puc-LacZ* activation in neurons is reduced (~37%) and GB cells show a progressive upregulation of *puc-LacZ* and a shift from neurons to GB cells from 63% *puc-LacZ* activation in glia 48h after the tumour induction to ~80% 96h after tumour induction (Figure 3A-D), indicating that JNK pathway is activated in GB cells progressively.

Timeline: GB first causes neurodegeneration, then TMs infiltrate and finally proliferates

To evaluate the progressive growth of the TMs and the number of glial cells, we dissected larval brains at 24, 48 and 72h after tumour induction (referred to as day 1D, 2D or 3 days in Figure 4A-C). To visualize and quantify the TMs network volume, we expressed a membrane-bound myristoylated Red Fluorescent Protein (*UAS-myrRFP*) in glial cells and to quantify the glial cell number we stained the glia nuclei with a specific anti-Repo antibody and obtained confocal images from whole brains (Figure 4A-C).

The statistical analysis of TMs volume (Figure 4D) shows no significant increase in the volume of the TM network between day 1 and day 2 after tumour induction. Nevertheless, there is a significant increase in the volume of the TMs between day 2 and day 3 after tumour induction. Similarly, the statistical analysis of the number of glial cells (Figure 4E) shows no significant increase in the number of glial cells between day 1 and day 2, but there is a significant increase between day 2 and day 3, and between day 1 and day 3 after tumour induction. This suggests a progressive growth and expansion of the TMs and a progressive increase in the number of glioma cells.

TMs are required in GB cells to mediate Wg signaling imbalance among neurons and GB cells. Wg signaling is upregulated in GB cells to promote proliferation, at expenses of the surrounding neurons in which the downregulation of the Wg pathway results in synapse loss, neurodegeneration and lethality.

To evaluate the impact of the progressive GB growth on the surrounding neurons, we quantified the number of synapses in the neuromuscular junction (NMJ) of third-instar larvae 1, 2 and 3 days after GB induction through immunofluorescence. NMJs were stained with anti-bruchpilot to reveal the synapses visualised by confocal microscopy (Figure 5A-C).

The statistical analysis of synapse number (Figure 5D) shows a progressive loss of synapse number between day 1 and day 2, and between day 2 and day 3 after tumour induction. The overall loss of synapses at the NMJ is highly significant (Figure 5D).

To determine whether there is an association between the volume of the network and the number of synapses at the NMJ, we plotted the number of synapses against the volume of the glial network in a correlation graph (Figure 5E). The correlation index is -0.966 (3s.f.) indicating there is a negative association between the volume of the TMs and the number of synapses at the NMJ. Therefore, larger TMs network leads to a greater synapse loss.

Discussion

Activating mutations for EGFR and PI3K pathways are the most frequent initial signals in GB. However, the attempts to treat GB reducing the activation of these pathways have so far been limited by acquired drug resistance. The current tendencies suggest that a multiple approach is required to obtain a more positive result (Taylor *et al.* 2012; Westphal *et al.* 2017; Prasad *et al.* 2011; Westhoff *et al.* 2014; Zhao *et al.* 2017). GB cells show a high mutation rate and usually present more than two sub-clones within the same patient and from the same primary tumour (McGranahan & Swanton 2017; Qazi *et al.* 2017).

Progressive tumour growth

Although there is an overall significant expansion in volume of the TMs and an increase in the number of glial cells in the *Drosophila* model of GB, between day 1 and day 2 of tumour development there is no significant increase for either parameters. Looking at the volume on day 2 after tumour induction there are some values above the average. There is also a large dispersion in volume and number of glial cells data in brains on day 3 after tumour induction. A possible explanation for this is that under physiological conditions, there is a stable state that prevents cells from exiting the cell cycle, proliferating or extending a network of TMs. Therefore, on day 1 after tumour induction, glioma cells do not show evident changes, there is a uniform range of values for the volume of TMs and number of glial cells. On day 2 after tumour induction, some individuals abandon this stable state and GB cells extend larger and longer TMs, although most individuals continue in stability and display morphological characteristics similar to control samples. However, on day 3 after tumour induction the development of the tumour causes changes that destabilise the situation leading to an increased expansion of TMs and higher proliferation of glial cells. Similar to GB patients, some individuals are more resistant than others to these changes, which would explain the variance in the values for network volume and number of glial cells on day 3 after tumour induction.

Progressive neurodegeneration

There is a significant progressive decrease in the number of synapses at the NMJ. Nevertheless, the variance in the number of synapses on day 1 after tumour induction is very large, reaching uniform values on days 2 and 3 after tumour induction. The individuals show different resistances to the changes caused by the GB, therefore, on day 1 after tumour induction, some individuals are largely affected by the tumour and suffer a great loss of synapses at the NMJ while other individuals are more resistant and maintain the number of synapses. On day 2 after tumour induction, the GB causes severe changes that affect all individuals in a similar manner regardless of their initial resistance.

We have observed a negative correlation between the volume of TMs and the number of synapses at the NMJ, suggesting that the TMs are responsible for the neurodegeneration. Previous studies from our laboratory have proved that TMs surround neurons and relocate Fz1 receptor in the area of contact, taking away WNT from the neurons (Portela *et al.* 2019), which leads to the degeneration of neurons (Rich & Bigner 2004). We can conclude that as the tumour progresses, it extends a network of TMs that grows progressively infiltrating in the brain and surrounding neurons depleting the ligand WNT from them and leading to their degeneration, process previously described as vampirization (Portela *et al.* 2019). The expansion of the TMs is slow during the first 24h of tumour development but increases after 48h of tumour development. The associated neurodegeneration is also progressive but is visible from the first 24h of tumour development.

Progressive activation of JNK pathway via Egr/Grnd

JNK signalling regulates MMPs expression in GB, which is required for TMs network formation and infiltration. Consequently, Wg pathway responds to JNK and TMs expansion, these three events conform a regulatory positive feedback loop in GB progression. Grnd is the receptor that interacts with the ligand Egr and activates JNK pathway in GB cells. GFP fused protein showed that Egr is produced in the surrounding neurons and accumulated in the membrane of GB TMs in contact with healthy neuronal tissue. The progressive activation of JNK pathway in glial cells correlate with the morphological changes (TM expansion and number of glial cells) that GB undergo after 48 of induction, and JNK pathway activation is essential for GB progression. Therefore, here is another example of neuron-glia molecular interaction which mediates the physiological status of the brain and the evolution of GB and reinforce the proposal of a bidirectional interaction between GB and surrounding healthy tissue. It is of interest to unravel the regulatory mechanisms that mediate *Egr* expression and secretion in neurons in response to GB induction, and the response in GB cells mediated by Grnd-Egr as a potential modulator for brain tumour advance.

Frizzled receptors in patients mediate matrix metalloproteinase MMP2 and MMP9 expression in different scenarios. Blocking WNT signalling, or MMP activity, reduces T cell migration through the basement membrane in vitro and into inflamed skin *in vivo*. MMP promoters respond to WNT signalling through tandem TCF sites and mediate T cell extravasation (Wu *et al.* 2007). MMP9 is a key molecular effector, downstream of HIF-1α and WNT activation, responsible for increased rates of neural stem cells proliferation and migration in hypoxia (Ingraham *et al.* 2011). In addition, *Mmp7* (also known as matrilysin) is a target gene of the WNT signalling pathway in lung epithelial cells and is known to be a key mediator of pulmonary fibrosis (Konigshoff *et al.* 2008). Moreover, MMPs expression is associated to GB invasion, growth and angiogenesis (Lakka *et al.* 2004; Rome *et al.* 2007). MMP2 and MMP9 co-silencing in combination with temozolomide treatment emerge as promising in the treatment against GB (Gabelloni *et al.* 2010).

The tandem JNK-Wg-TMs trigger the expression of *MMPs* in *Drosophila* GB cells. Fly MMP1 and MMP2 degrade the ECM and, in the brain facilitate the infiltration of TMs. MMPs are upregulated in human patients (Hagemann *et al.* 2012) as well as in *Drosophila* GB model. Besides, MMPs expression attenuation reduces the volume occupied by TMs and Wg signalling with the concomitant consequences: reduction of GB progression, prevention of neurodegeneration (synapse loss) and lethality. Consequently, MMPs are part of the positive feedback loop in GB and mediate the equilibrium among Wg signalling, JNK and TMs expansion (Portela *et al.* 2019).

MMPs have been of interest for GB studies for more than a decade, numerous studies correlate MMPs expression with a poor prognosis (Hagemann *et al.* 2012; Xue *et al.* 2017) but the precise mechanisms mediating the cellular impact of MMPs and the regulation of *MMPs* expression was unknown. We hypothesize that GB cells become addicted to the positive feedback loop formed by Wg pathway, JNK, MMPs and the TMs, and then become independent of the founder mutations (PI3K and EGFR). Therefore, treatments tackling EGFR of PI3K failed to success as GB cells rely of other inputs. This particular signalling

loop is required for GB cells to progress but is dispensable for normal glia development (Portela *et al.* 2019) which puts these discoveries as targetable features for GB treatments.

Finally, the specific targets of MMPs will be of interest to determine which ECM components are essential to prevent TMs expansion. There are two MMPs in *Drosophila* (MMP1 and MMP2) with 10 and 3 isoforms respectively, MMP1 and MMP2 have been classically differentiated by their extracellular or membrane associated localization, however this concept is currently under debate (LaFever *et al.* 2017). It is proposed that each MMP has particular targets from the ECM which are sensible of degradation, and recent classifications have brought light on the specificity of each protease and the different substrates (Hagemann *et al.* 2012). Our previous results show that the attenuation of either MMP1 or MMP2 prevents GB progression (Portela *et al.* 2019), thus the potential substrates and the functional implications for GB need to be established in future studies.

Acknowledgements

We thank Professor Alberto Ferrús for helpful discussions. We are grateful to R. Read, I. Guerrero, P. Leopold, , E. Martín-Blanco, E. Moreno, the Bloomington *Drosophila* stock Centre and the Developmental Studies Hydridoma Bank for supplying fly stocks and antibodies, and FlyBase for its wealth of information. We acknowledge the support of the Confocal Microscopy unit and Molecular Biology unit at the Cajal Institute for their help with this project. MP holds a fellowship from the Juan de la Cierva program IJCI-2014-19272 and SCT holds a contract from the Ramón y Cajal program RYC-2012-11410 from the Spanish MICINN. Research has been funded by grant BFU2015-65685P. Authors declare no conflicts of interest.

Experimental Procedures

Fly stocks

Flies were raised in standard fly food at 25ºC. Fly stocks from the Bloomington stock Centre: *UAS-lacZ* (BL8529)*, UAS-myr-RFP* (BL7119), *repo-Gal4* (BL7415)*, tub-gal80^{ts}* (BL7019), Egr-GFP (BL66381) *UAS-dEGFR$^{\lambda}$, UAS-PI3K92E* (dp110^{CAAX}) (A gift from R. Read), *UAS-ihog-RFP* (a gift from I. Guerrero), *puc-lacZ* (a gift from E. Martín-Blanco), *UAS-dmyc (Moreno & Basler 2004), UAS-TOR-DER^{CA}(Dominguez et al. 1998)*.

Drosophila glioblastoma model

The most frequent genetic lesions in human gliomas include mutation or amplification of the Epidermal Growth Factor Receptor (EGFR) gene. Glioma-associated EGFR mutant forms show constitutive kinase activity that chronically stimulates Ras signaling to drive cell proliferation and migration (Furnari *et al.* 2007; Maher *et al.* 2001). Other common genetic lesions include loss of the lipid phosphatase PTEN, which antagonizes the phosphatidylinositol-3 kinase (PI3K) signaling pathway, and mutations that activate PI3KCA, which encodes the p110a catalytic subunit of PI3K [98-99]. Gliomas often show constitutively active Akt, a major PI3K effector. However, EGFR-Ras or PI3K mutations alone are not sufficient to transform glial cells. Instead, multiple mutations that coactivate EGFR-Ras and PI3K/Akt pathways are required to induce a glioma (Holland 2000). In *Drosophila*, a combination of EGFR and PI3K mutations effectively causes a glioma-like condition that shows features of human gliomas including glia expansion, brain invasion, neuron dysfunction, synapse loss and neurodegeneration (Read *et al.* 2009; Kegelman *et al.* 2014; Read 2011). Moreover, this model has proved to be useful in finding new kinase activities relevant to glioma progression.(Read *et al.* 2009) To generate a glioma in *Drosophila*

melanogaster adult flies, the Gal4/UAS system (Brand & Perrimon 1993) was used as described above (*repo*-Gal4>UAS-*EGFRλ*,UAS-*dp110*. To restrict the expression of this genetic combination and control it in a temporal manner, we used the thermo sensitive repression system Gal80^{TS}. Individuals maintained at 17ºC did not activate the expression of the UAS constructs, but when the larvae were switched to 29ºC, the protein Gal80^{TS} changed conformation and was not longer able to bind to Gal4 to prevent its interaction with UAS sequences, and the expression system was activated and therefore the GB was induced.

Antibodies for Immunofluorescence

Third-instar larval brains, were dissected in phosphate-buffered saline (PBS), fixed in 4% formaldehyde for 30min, washed in PBS + 0.1 or 0.3% Triton X-100 (PBT), and blocked in PBT + 5% BSA.

Antibodies used were: mouse anti-Wg (DSHB 1:50), mouse anti-Repo (DSHB 1:50), mouse anti-Fz1 (DSHB 1:50), mouse anti-Cyt-Arm (DSHB 1:50), mouse anti-MMP1 (DSHB 5H7B11, 3A6B4, 3B8D12, 1:50), guinea pig anti-grnd (Andersen *et al.* 2015) (1:250, P. Leopold), mouse anti-β-galactosidase (Sigma, 1:500), mouse anti-GFP (Invitrogen A11120, 1:500), mouse anti-bruchpilot (DSHB Nc82, 1:20), Rabbit anti-Hrp (Jackson Immunoresearch 111-035-144, 1:400).

Secondary antibodies: anti-mouse Alexa 488, 568, 647, anti-rabbit Alexa 488, 568, 647 (Thermofisher, 1:500). DNA was stained with 2-(4-amidinophenyl)-1H-indole-6-carboxamidine (DAPI, 1µM).

Imaging

Fluorescent labeled samples were mounted in Vectashield mounting media with DAPI (Vector Laboratories) and analyzed by Confocal microscopy (LEICA TCS SP5). Images were processed using Leica LAS AF Lite and Fiji (Image J 1.50e). Images were assembled using Adobe Photoshop CS5.1.

Quantifications

Relative MMP1 and grnd staining within brains was determined from images taken at the same confocal settings. Average pixel intensity was measured using measurement log tool from Fiji 1.51g and Adobe Photoshop CS5.1. Average pixel intensity was measured in the glial tissue and in the adjacent neuronal tissue (N<10 for each sample) and expressed as a Glia/Neuron ratio. Glial network volume was quantified using Imaris surface tool (Imaris 6.3.1 Bitplane Scientific Solutions software).

The number of $Repo^{+}$ cells, the number of synaptic active sites and the number of puc-lacZ positive cells was quantified by using the spots tool Imaris 6.3.1 software, we selected a minimum size and threshold for the puncta in the control samples of each experiment. Then we applied these conditions to the analysis of each corresponding experimental sample. For the puc-lacZ glia or neuron co-localization studies we quantified the total number of puc-$lacZ^{+}$ cells and then applied a co-localization filter (intensity center of the channel of interest) using the Spots tool from the Imaris 6.3.1 software.

For the co-localization of Egr-GFP in glial cells, GFP channel volume was quantified using Imaris surface tool. We selected a specific threshold for the total volume in the control samples and then we applied these conditions to the analysis of the corresponding experimental sample. Then we applied a co-localization filter (intensity mean of the red channel)

Statistical Analysis

To analyze and plot the data, we used Microsoft Excel 2013 and GraphPad Prism 6. We performed a D'Agostino & Pearson normality test and the data found to have a normal distribution were analyzed by a two-tailed t test with Welch-correction. In the case of multiple comparisons, we used a One-way ANOVA with Bonferroni post-test. The data that did not pass the normality test were subjected to a two-tailed Mann–Whitney U test or in the case of multiple comparisons a Kruskal–Wallis test with Dunns post-test. Error bars represent standard error of the mean. * represents p value ≤ 0.05; ** p value ≤ 0.01; *** p value ≤ 0.001. Statistical values of p value >0.05 were not considered significant, (n.s.).

Figure Legends

Figure 1: Independent constitutive activation of PI3K or EGFR or ectopic *dmyc* are not responsible for MMP1 accumulation.

Brains from 3rd instar larvae. Glia are labeled with *UAS-Ihog-RFP* driven by *repo-Gal4* to visualize active cytonemes/ TM structures in glial cells and stained with MMP1 (green). (A) MMP1 (green) is homogeneously distributed in control. (B) In Glioma brains, MMP1 accumulates in the TMs and specifically in the TM projections that are in contact with the neuronal clusters. (C-E) MMP1 (green) is homogeneously distributed in (B) $dp110^{CAAX}$, (C)$TOR\text{-}DER^{CA}$ and (D) *dmyc* sections. The glial cytonemes (red) revealed by Ihog-RFP do not overgrow or encapsulate neuronal clusters. Nuclei are marked with DAPI (blue). (F)

Quantification of MMP1 staining ratio between iHog^{+} and iHog^{-} domains. Kruskal–Wallis test with Dunns post-test. Error bars show S.D. *** P<0.001 or ns for non-significant. Scale bar size is indicated in this and all figures.

Genotypes:

(A) *UAS-lacZ/repo-Gal4, UAS-ihog-RFP*
(B) *UAS-dEGFR$^{\lambda}$, UAS-dp110^{CAAX};; repo-Gal4, UAS-ihog-RFP*
(C) *UAS-dp110^{CAAX};; repo-Gal4, UAS-ihog-RFP*
(D) *UAS-TOR-DER^{CA} ;; repo-Gal4, UAS-ihog-RFP*
(E) *repo-Gal4, UAS-ihog-RFP/UAS-dmyc*

Figure 2: Egr and its receptor Grindelwald accumulate in GB

Brains from 3rd instar larvae. Glia are labeled with *UAS-Ihog-RFP* driven by *repo-Gal4* to visualize active cytonemes/ TM structures in glial cells, carry a Egr-GFP reporter (green). (A-B) In control brain sections Egr-GFP (green) signal is localized mostly (70%) in neurons in close contact with glial cells. (C-D) In glioma brain sections Egr-GFP (green) signal shifts and it is 50% localized in glioma cells. (E) Quantification of the percentage of Egr in glia in control and glioma samples. (F-G) grnd staining (green) in control and glioma samples. (H) Quantification of the grnd pixel intensity. Nuclei are marked with DAPI (blue). Two-tailed t test with Welch-correction. Error bars show S.D. * P<0.05, ***p≤0.001 . Scale bar size are indicated in this and all figures.

Genotypes:

(A-B) Egr-GFP; *repo-Gal4, ihog-RFP/UAS-lacZ*
(C-D) *UAS-dEGFR$^{\lambda}$, UAS-dp110^{CAAX};Egr-GFP; repo-Gal4, UAS-ihog-RFP*
(F) *repo-Gal4, ihog-RFP/UAS-lacZ*
(G) *UAS-dEGFR$^{\lambda}$, UAS-dp110^{CAAX};; repo-Gal4, UAS-ihog-RFP*

Figure 3: JNK signaling pathway activation in glioma

Larval brain sections from 3rd instar larvae displayed at the same scale. Glial cell bodies and membranes are labeled with *UAS-myr-RFP* (red) driven by *repo-Gal4* (A-C) JNK signaling pathway reporter *puc-lacZ* in control, glioma 48h and glioma 96h after tumour induction. *puc-*

lacZ shows activation of the pathway mostly in neurons in control samples (A) and then shows a progressive activation in GB cells (B-C). (D) Quantification of the % of cells with *puc-lacZ* activation in glial cells and neurons. Nuclei are marked with DAPI (blue). One-way ANOVA with Bonferroni post-test. Error bars show S.D. ** P<0.01, *** P<0.001. Scale bar size is indicated in this and all figures.

Genotypes:

(A) *Gal80^{ts}/repo-Gal4, myr-RFP/puc-lacZ*
(B-C) *Gal80^{ts}/UAS-dEGFR$^{\lambda}$, UAS-dp110^{CAAX};; repo-Gal4, myr-RFP/puc-lacZ*

Figure 4. GB TM network volume and number of glial cells 1, 2 and 3 days after tumour induction. Third-instar larval brains or optical lobes Repo+ cells (glial cells) are marked with anti-Repo and visualised as green spots. TMs are marked in red via *UAS-myrRFP* which accumulated RFP in the plasma membrane of glial cells. (A) Third-instar larval brain 1 day after tumour induction. (B) Third-instar larval brain 2 days after tumour induction. (C) Third-instar larval brain 3 days after tumour induction. (D) Graphical representation of the TM volume at the different timepoints after tumour induction. (E) Graphical representation of the number of glial cells in brains at the different timepoints after tumour induction. Nuclei are marked with DAPI (blue). One-way ANOVA with Bonferroni post-test. *p≤0.05 **p≤0.01, n.s.=not significant.

Genotypes:

(A-C) *UAS-dEGFR$^{\lambda}$, UAS-dp110^{CAAX}; Gal80^{ts}; repo-Gal4, myr-RFP*

Figure 5. Number of synapses at the NMJ of third-instar larvae 1, 2 and 3 days after tumour induction. The synaptic connexions at the NMJ of *Drosophila* larvae are between muscles 6 and 7 in the third and fourth abdominal segment. Anti-Bruchpilot (α-NC82) binds to Bruchpilot marking presynaptic zones in green. Anti-Hrp marks the neuron membrane in blue. Glial cells are visualised in red via *UAS-myrRFP* which accumulates RFP in the glial membrane. (A) Third-instar larval NMJ 1 day after tumour induction. (B) Third-instar larval

NMJ 2 days after tumour induction. (C) Third-instar larval NMJ 3 days after tumour induction. (D) Graphical representation of the number of synapses at the NMJ 1, 2 and 3 days after tumour induction. One-way ANOVA with Bonferroni post-test. ***p≤0.001, * p≤0.05. (E) Scatter plot showing the correlation between volume of the TMs and number of synapses at the NMJ. There is a negative correlation between the volume of the network and the number of synapses, therefore, at smaller volumes of glial network there are more synaptic connexions at the NMJ and as the volume increases, more synapses are lost.

Genotypes:

(A-C) *UAS-dEGFR$^{\lambda}$, UAS-dp110^{CAAX}; Gal80^{ts}; repo-Gal4, myr-RFP*

Figure S1: Independent constitutive activation of PI3K or EGFR or ectopic *dmyc* are not responsible for Wg/Fz1 accumulation and expansion of TM network.

Brains from 3rd instar larvae. Glia are labeled with *UAS-Ihog-RFP* driven by *repo-Gal4* to visualize active cytonemes/ TM structures in glial cells and stained with Fz1/Wg or Cyt-Arm (green). (A-E) Fz1 (green) is homogeneously distributed in control (A). (B) Fz1 accumulates in the TMs in glioma brains. Fz1 is homogeneously distributed in (B) *dp110^{CAAX},* (C)*TOR-DER^{CA}* and (D) *dmyc* sections similar to the control (A). (F-K) Wg and Cyt-Arm (green) are homogeneously distributed in control brain sections (F, I) as well as in *dmyc* sections (G, J) and the glial network shown in red by Ihog-RFP does not overgrow or encapsulate neuronal clusters as opposed to GB brains where Wg accumulates in TMs (G) and Cyt-Arm accumulates in the neurons' cytoplasm where it is inactive (J). Nuclei are marked with DAPI.

Genotypes:

(A, F, I) *UAS-lacZ/repo-Gal4, UAS-ihog-RFP*

(B, G, J) *UAS-dEGFR$^{\lambda}$, UAS-dp110^{CAAX};; repo-Gal4, UAS-ihog-RFP*

(C) *UAS-dp110^{CAAX};; repo-Gal4, UAS-ihog-RFP*

(D) *UAS-TOR-DER^{CA} ;; repo-Gal4, UAS-ihog-RFP*

(E, H, K) *repo-Gal4, UAS-ihog-RFP/UAS-dmyc*

References

Alifieris, C. and Trafalis, D. T. (2015) Glioblastoma multiforme: Pathogenesis and treatment. *Pharmacol Ther* **152,** 63-82.

Andersen, D. S., Colombani, J., Palmerini, V. et al. (2015) The Drosophila TNF receptor Grindelwald couples loss of cell polarity and neoplastic growth. *Nature* **522,** 482-486.

Annibali, D., Whitfield, J. R., Favuzzi, E. et al. (2014) Myc inhibition is effective against glioma and reveals a role for Myc in proficient mitosis. *Nat Commun* **5,** 4632.

Arnes, M. and Casas Tinto, S. (2017) Aberrant Wnt signaling: a special focus in CNS diseases. *J Neurogenet* **31,** 216-222.

Brand, A. H. and Perrimon, N. (1993) Targeted gene expression as a means of altering cell fates and generating dominant phenotypes. *Development* **118,** 401-415.

Casas-Tinto, S. and Portela, M. (2019) Cytonemes, Their Formation, Regulation, and Roles in Signaling and Communication in Tumorigenesis. *Int J Mol Sci* **20**.

Chatterjee, N. and Bohmann, D. (2012) A versatile PhiC31 based reporter system for measuring AP-1 and Nrf2 signaling in Drosophila and in tissue culture. *PLoS One* **7,** e34063.

Chen, W., Zhong, X., Wei, Y., Liu, Y., Yi, Q., Zhang, G., He, L., Chen, F. and Luo, J. (2016) TGF-beta Regulates Survivin to Affect Cell Cycle and the Expression of EGFR and MMP9 in Glioblastoma. *Mol Neurobiol* **53,** 1648-1653.

Cheng, C. Y., Hsieh, H. L., Hsiao, L. D. and Yang, C. M. (2012) PI3-K/Akt/JNK/NF-kappaB is essential for MMP-9 expression and outgrowth in human limbal epithelial cells on intact amniotic membrane. *Stem Cell Res* **9,** 9-23.

de Lucas, A. G., Schuhmacher, A. J., Oteo, M. et al. (2016) Targeting MT1-MMP as an ImmunoPET-Based Strategy for Imaging Gliomas. *PLoS One* **11,** e0158634.

Dominguez, M., Wasserman, J. D. and Freeman, M. (1998) Multiple functions of the EGF receptor in Drosophila eye development. *Curr Biol* **8,** 1039-1048.

Feng, J., Yan, P. F., Zhao, H. Y., Zhang, F. C., Zhao, W. H. and Feng, M. (2016) Inhibitor of Nicotinamide Phosphoribosyltransferase Sensitizes Glioblastoma Cells to Temozolomide via Activating ROS/JNK Signaling Pathway. *Biomed Res Int* **2016,** 1450843.

Furnari, F. B., Fenton, T., Bachoo, R. M. et al. (2007) Malignant astrocytic glioma: genetics, biology, and paths to treatment. *Genes Dev* **21,** 2683-2710.

Gabelloni, P., Da Pozzo, E., Bendinelli, S. et al. (2010) Inhibition of metalloproteinases derived from tumours: new insights in the treatment of human glioblastoma. *Neuroscience* **168,** 514-522.

Gallego, O. (2015) Nonsurgical treatment of recurrent glioblastoma. *Curr Oncol* **22,** e273-281.

Hagemann, C., Anacker, J., Ernestus, R. I. and Vince, G. H. (2012) A complete compilation of matrix metalloproteinase expression in human malignant gliomas. *World J Clin Oncol* **3,** 67-79.

Hagemann, C., Anacker, J., Haas, S., Riesner, D., Schomig, B., Ernestus, R. I. and Vince, G. H. (2010) Comparative expression pattern of Matrix-Metalloproteinases in human glioblastoma cell-lines and primary cultures. *BMC Res Notes* **3,** 293.

Hagemann, T., Wilson, J., Kulbe, H. et al. (2005) Macrophages induce invasiveness of epithelial cancer cells via NF-kappa B and JNK. *J Immunol* **175,** 1197-1205.

Hayden, E. C. (2010) Genomics boosts brain-cancer work. *Nature* **463,** 278.

Holland, E. C. (2000) Glioblastoma multiforme: the terminator. *Proc Natl Acad Sci U S A* **97,** 6242-6244.

Hsu, J. B., Chang, T. H., Lee, G. A., Lee, T. Y. and Chen, C. Y. (2019) Identification of potential biomarkers related to glioma survival by gene expression profile analysis. *BMC Med Genomics* **11,** 34.

Huang, C., Rajfur, Z., Borchers, C., Schaller, M. D. and Jacobson, K. (2003) JNK phosphorylates paxillin and regulates cell migration. *Nature* **424,** 219-223.

Igaki, T., Kanda, H., Yamamoto-Goto, Y., Kanuka, H., Kuranaga, E., Aigaki, T. and Miura, M. (2002) Eiger, a TNF superfamily ligand that triggers the Drosophila JNK pathway. *EMBO J* **21,** 3009-3018.

Ingraham, C. A., Park, G. C., Makarenkova, H. P. and Crossin, K. L. (2011) Matrix metalloproteinase (MMP)-9 induced by Wnt signaling increases the proliferation and migration of embryonic neural stem cells at low O2 levels. *J Biol Chem* **286,** 17649-17657.

Ispanovic, E. and Haas, T. L. (2006) JNK and PI3K differentially regulate MMP-2 and MT1-MMP mRNA and protein in response to actin cytoskeleton reorganization in endothelial cells. *Am J Physiol Cell Physiol* **291,** C579-588.

Jarabo, P., de Pablo, C., Herranz, H., Martin, F. A. and Casas-Tinto, S. (2020).

Jemc, J. C., Milutinovich, A. B., Weyers, J. J., Takeda, Y. and Van Doren, M. (2012) raw Functions through JNK signaling and cadherin-based adhesion to regulate Drosophila gonad morphogenesis. *Dev Biol* **367,** 114-125.

Kamino, M., Kishida, M., Kibe, T. et al. (2011) Wnt-5a signaling is correlated with infiltrative activity in human glioma by inducing cellular migration and MMP-2. *Cancer Sci* **102,** 540-548.

Kegelman, T. P., Hu, B., Emdad, L., Das, S. K., Sarkar, D. and Fisher, P. B. (2014) In vivo modeling of malignant glioma: the road to effective therapy. *Adv Cancer Res* **121,** 261-330.

Kitanaka, C., Sato, A. and Okada, M. (2013) JNK Signaling in the Control of the Tumor-Initiating Capacity Associated with Cancer Stem Cells. *Genes Cancer* **4,** 388-396.

Konigshoff, M., Balsara, N., Pfaff, E. M., Kramer, M., Chrobak, I., Seeger, W. and Eickelberg, O. (2008) Functional Wnt signaling is increased in idiopathic pulmonary fibrosis. *PLoS One* **3,** e2142.

LaFever, K. S., Wang, X., Page-McCaw, P., Bhave, G. and Page-McCaw, A. (2017) Both Drosophila matrix metalloproteinases have released and membrane-tethered forms but have different substrates. *Sci Rep* **7,** 44560.

Lakka, S. S., Gondi, C. S., Yanamandra, N., Olivero, W. C., Dinh, D. H., Gujrati, M. and Rao, J. S. (2004) Inhibition of cathepsin B and MMP-9 gene expression in glioblastoma cell line via RNA interference reduces tumor cell invasion, tumor growth and angiogenesis. *Oncogene* **23,** 4681-4689.

Langen, M., Koch, M., Yan, J., De Geest, N., Erfurth, M. L., Pfeiffer, B. D., Schmucker, D., Moreau, Y. and Hassan, B. A. (2013) Mutual inhibition among postmitotic neurons regulates robustness of brain wiring in Drosophila. *Elife* **2,** e00337.

Lee, Y. S., Lan Tran, H. T. and Van Ta, Q. (2009) Regulation of expression of matrix metalloproteinase-9 by JNK in Raw 264.7 cells: presence of inhibitory factor(s) suppressing MMP-9 induction in serum and conditioned media. *Exp Mol Med* **41,** 259-268.

Louis, D. N., Perry, A., Reifenberger, G. et al. (2016) The 2016 World Health Organization Classification of Tumors of the Central Nervous System: a summary. *Acta Neuropathol* **131,** 803-820.

Lowy, A. M., Clements, W. M., Bishop, J., Kong, L., Bonney, T., Sisco, K., Aronow, B., Fenoglio-Preiser, C. and Groden, J. (2006) beta-Catenin/Wnt signaling regulates expression of the membrane type 3 matrix metalloproteinase in gastric cancer. *Cancer Res* **66,** 4734-4741.

Lyu, J. and Joo, C. K. (2005) Wnt-7a up-regulates matrix metalloproteinase-12 expression and promotes cell proliferation in corneal epithelial cells during wound healing. *J Biol Chem* **280,** 21653-21660.

Maher, E. A., Furnari, F. B., Bachoo, R. M., Rowitch, D. H., Louis, D. N., Cavenee, W. K. and DePinho, R. A. (2001) Malignant glioma: genetics and biology of a grave matter. *Genes Dev* **15,** 1311-1333.

Malemud, C. J. (2006) Matrix metalloproteinases (MMPs) in health and disease: an overview. *Front Biosci* **11,** 1696-1701.

Martin-Blanco, E., Gampel, A., Ring, J., Virdee, K., Kirov, N., Tolkovsky, A. M. and Martinez-Arias, A. (1998) puckered encodes a phosphatase that mediates a feedback loop regulating JNK activity during dorsal closure in Drosophila. *Genes Dev* **12,** 557-570.

Matsuda, K., Sato, A., Okada, M. et al. (2012) Targeting JNK for therapeutic depletion of stem-like glioblastoma cells. *Sci Rep* **2,** 516.

McGranahan, N. and Swanton, C. (2017) Clonal Heterogeneity and Tumor Evolution: Past, Present, and the Future. *Cell* **168,** 613-628.

McGuire, S. (2016) World Cancer Report 2014. Geneva, Switzerland: World Health Organization, International Agency for Research on Cancer, WHO Press, 2015. *Adv Nutr* **7,** 418-419.

Miller, J. J., Shih, H. A., Andronesi, O. C. and Cahill, D. P. (2017) Isocitrate dehydrogenase-mutant glioma: Evolving clinical and therapeutic implications. *Cancer* **123,** 4535-4546.

Moreno, E. and Basler, K. (2004) dMyc transforms cells into super-competitors. *Cell* **117,** 117-129.

Moreno, E., Yan, M. and Basler, K. (2002) Evolution of TNF signaling mechanisms: JNK-dependent apoptosis triggered by Eiger, the Drosophila homolog of the TNF superfamily. *Curr Biol* **12,** 1263-1268.

Mu, N., Gu, J., Liu, N. et al. (2018) PRL-3 is a potential glioblastoma prognostic marker and promotes glioblastoma progression by enhancing MMP7 through the ERK and JNK pathways. *Theranostics* **8,** 1527-1539.

Munaut, C., Noel, A., Hougrand, O., Foidart, J. M., Boniver, J. and Deprez, M. (2003) Vascular endothelial growth factor expression correlates with matrix metalloproteinases MT1-MMP, MMP-2 and MMP-9 in human glioblastomas. *Int J Cancer* **106,** 848-855.

Nakada, M., Okada, Y. and Yamashita, J. (2003) The role of matrix metalloproteinases in glioma invasion. *Front Biosci* **8,** e261-269.

Okada, M., Sato, A., Shibuya, K. et al. (2014) JNK contributes to temozolomide resistance of stem-like glioblastoma cells via regulation of MGMT expression. *Int J Oncol* **44,** 591-599.

Osswald, M., Jung, E., Sahm, F. et al. (2015) Brain tumour cells interconnect to a functional and resistant network. *Nature* **528,** 93-98.

Osswald, M., Solecki, G., Wick, W. and Winkler, F. (2016) A malignant cellular network in gliomas: potential clinical implications. *Neuro Oncol* **18,** 479-485.

Page-McCaw, A., Serano, J., Sante, J. M. and Rubin, G. M. (2003) Drosophila matrix metalloproteinases are required for tissue remodeling, but not embryonic development. *Dev Cell* **4,** 95-106.

Portela, M., Venkataramani, V., Fahey-Lozano, N., Seco, E., Losada-Perez, M., Winkler, F. and Casas-Tinto, S. (2019) Glioblastoma cells vampirize WNT from neurons and trigger a JNK/MMP signaling loop that enhances glioblastoma progression and neurodegeneration. *PLoS Biol* **17,** e3000545.

Prasad, G., Sottero, T., Yang, X. et al. (2011) Inhibition of PI3K/mTOR pathways in glioblastoma and implications for combination therapy with temozolomide. *Neuro Oncol* **13,** 384-392.

Qazi, M. A., Vora, P., Venugopal, C., Sidhu, S. S., Moffat, J., Swanton, C. and Singh, S. K. (2017) Intratumoral heterogeneity: pathways to treatment resistance and relapse in human glioblastoma. *Ann Oncol* **28,** 1448-1456.

Read, R. D. (2011) Drosophila melanogaster as a model system for human brain cancers. *Glia* **59,** 1364-1376.

Read, R. D., Cavenee, W. K., Furnari, F. B. and Thomas, J. B. (2009) A drosophila model for EGFR-Ras and PI3K-dependent human glioma. *PLoS Genet* **5,** e1000374.

Rich, J. N. and Bigner, D. D. (2004) Development of novel targeted therapies in the treatment of malignant glioma. *Nat Rev Drug Discov* **3,** 430-446.

Rogers, T. W., Toor, G., Drummond, K., Love, C., Field, K., Asher, R., Tsui, A., Buckland, M. and Gonzales, M. (2018) The 2016 revision of the WHO Classification of Central Nervous System

Tumours: retrospective application to a cohort of diffuse gliomas. *J Neurooncol* **137,** 181-189.

Rome, C., Arsaut, J., Taris, C., Couillaud, F. and Loiseau, H. (2007) MMP-7 (matrilysin) expression in human brain tumors. *Mol Carcinog* **46,** 446-452.

Roomi, M. W., Kalinovsky, T., Rath, M. and Niedzwiecki, A. (2017) Modulation of MMP-2 and MMP-9 secretion by cytokines, inducers and inhibitors in human glioblastoma T-98G cells. *Oncol Rep* **37,** 1907-1913.

Roth, W., Wild-Bode, C., Platten, M., Grimmel, C., Melkonyan, H. S., Dichgans, J. and Weller, M. (2000) Secreted Frizzled-related proteins inhibit motility and promote growth of human malignant glioma cells. *Oncogene* **19,** 4210-4220.

Ruan, W., Srinivasan, A., Lin, S., Kara k, I. and Barker, P. A. (2016) Eiger-induced cell death relies on Rac1-dependent endocytosis. *Cell Death Dis* **7,** e2181.

Tateishi, K., Iafrate, A. J., Ho, Q. et al. (2016) Myc-Driven Glycolysis Is a Therapeutic Target in Glioblastoma. *Clin Cancer Res* **22,** 4452-4465.

Taylor, T. E., Furnari, F. B. and Cavenee, W. K. (2012) Targeting EGFR for treatment of glioblastoma: molecular basis to overcome resistance. *Curr Cancer Drug Targets* **12,** 197-209.

Uhlirova, M. and Bohmann, D. (2006) JNK- and Fos-regulated Mmp1 expression cooperates with Ras to induce invasive tumors in Drosophila. *EMBO J* **25,** 5294-5304.

Uraguchi, M., Morikawa, M., Shirakawa, M., Sanada, K. and Imai, K. (2004) Activation of WNT family expression and signaling in squamous cell carcinomas of the oral cavity. *J Dent Res* **83,** 327-332.

Veeravalli, K. K. and Rao, J. S. (2012) MMP-9 and uPAR regulated glioma cell migration. *Cell Adh Migr* **6,** 509-512.

Waitkus, M. S., Diplas, B. H. and Yan, H. (2018) Biological Role and Therapeutic Potential of IDH Mutations in Cancer. *Cancer Cell* **34,** 186-195.

Wang, X., Huang, Z., Wu, Q. et al. (2017) MYC-Regulated Mevalonate Metabolism Maintains Brain Tumor-Initiating Cells. *Cancer Res* **77,** 4947-4960.

Westhoff, M. A., Karpel-Massler, G., Bruhl, O., Enzenmuller, S., La Ferla-Bruhl, K., Siegelin, M. D., Nonnenmacher, L. and Debatin, K. M. (2014) A critical evaluation of PI3K inhibition in Glioblastoma and Neuroblastoma therapy. *Mol Cell Ther* **2,** 32.

Westphal, M., Maire, C. L. and Lamszus, K. (2017) EGFR as a Target for Glioblastoma Treatment: An Unfulfilled Promise. *CNS Drugs* **31,** 723-735.

Wick, W., Osswald, M., Wick, A. and Winkler, F. (2018) Treatment of glioblastoma in adults. *Ther Adv Neurol Disord* **11,** 1756286418790452.

Wu, B., Crampton, S. P. and Hughes, C. C. (2007) Wnt signaling induces matrix metalloproteinase expression and regulates T cell transmigration. *Immunity* **26,** 227-239.

Xue, Q., Cao, L., Chen, X. Y., Zhao, J., Gao, L., Li, S. Z. and Fei, Z. (2017) High expression of MMP9 in glioma affects cell proliferation and is associated with patient survival rates. *Oncol Lett* **13,** 1325-1330.

Yamamoto, M., Ueno, Y., Hayashi, S. and Fukushima, T. (2002) The role of proteolysis in tumor invasiveness in glioblastoma and metastatic brain tumors. *Anticancer Res* **22,** 4265-4268.

Zeigler, M. E., Chi, Y., Schmidt, T. and Varani, J. (1999) Role of ERK and JNK pathways in regulating cell motility and matrix metalloproteinase 9 production in growth factor-stimulated human epidermal keratinocytes. *J Cell Physiol* **180,** 271-284.

Zeng, A., Yin, J., Li, Y. et al. (2018) miR-129-5p targets Wnt5a to block PKC/ERK/NF-kappaB and JNK pathways in glioblastoma. *Cell Death Dis* **9,** 394.

Zhao, H. F., Wang, J., Shao, W., Wu, C. P., Chen, Z. P., To, S. T. and Li, W. P. (2017) Recent advances in the use of PI3K inhibitors for glioblastoma multiforme: current preclinical and clinical development. *Mol Cancer* **16,** 100.

Figure 1

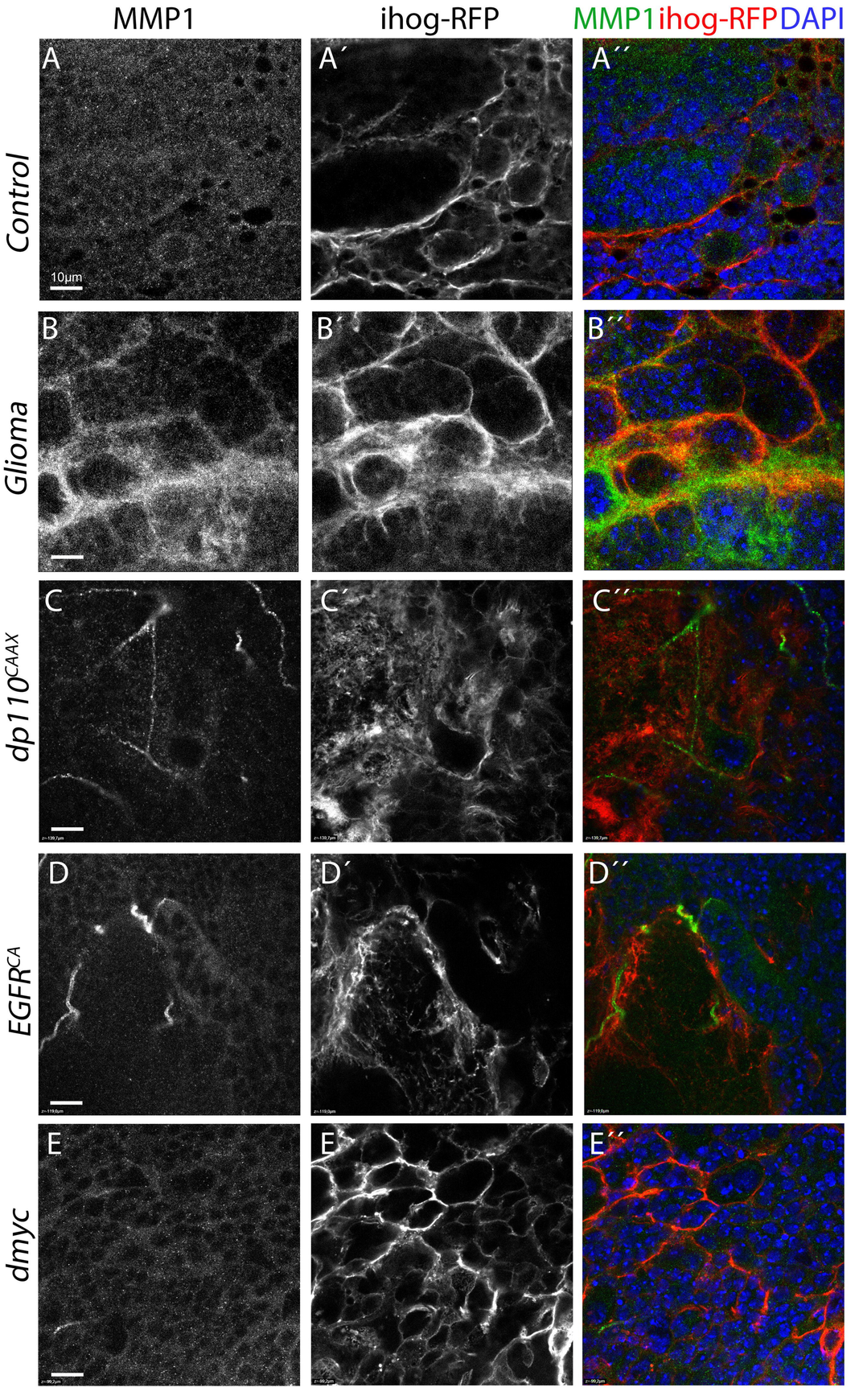

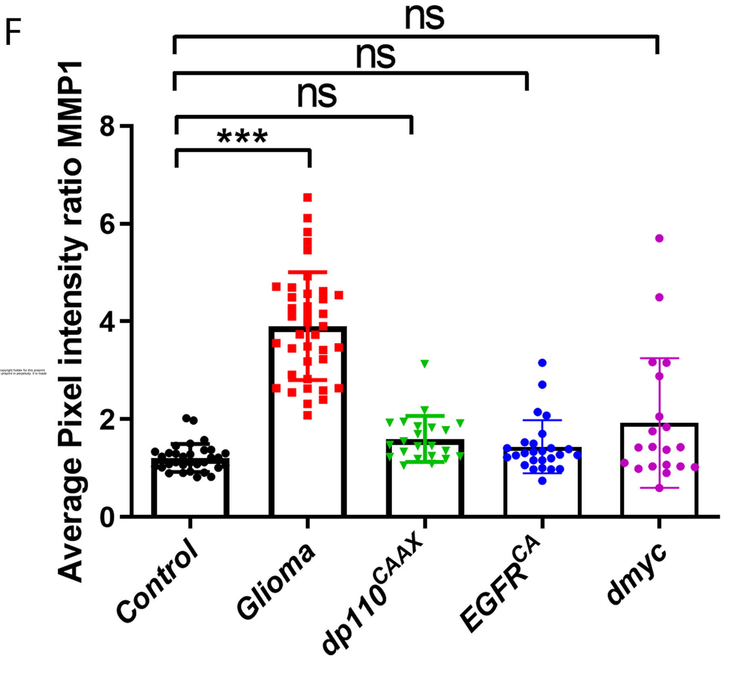

Figure 2

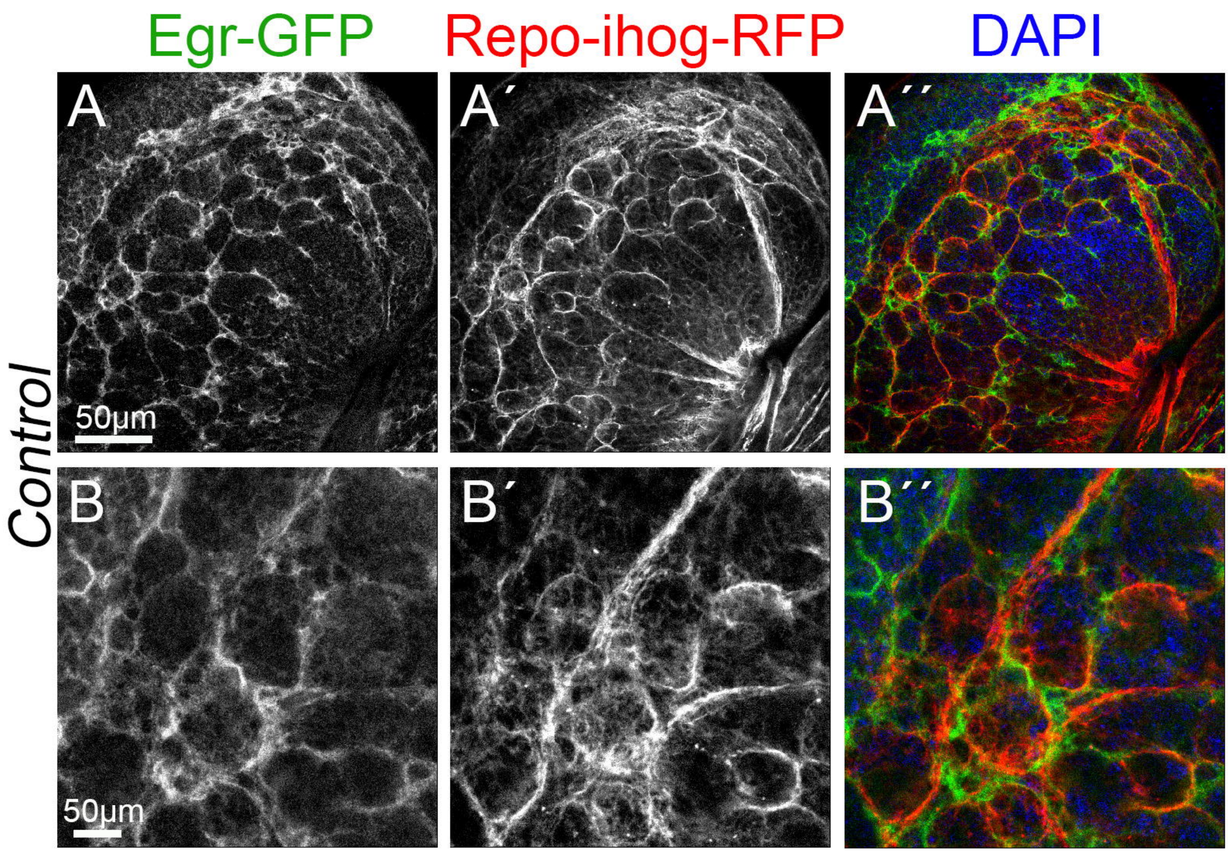

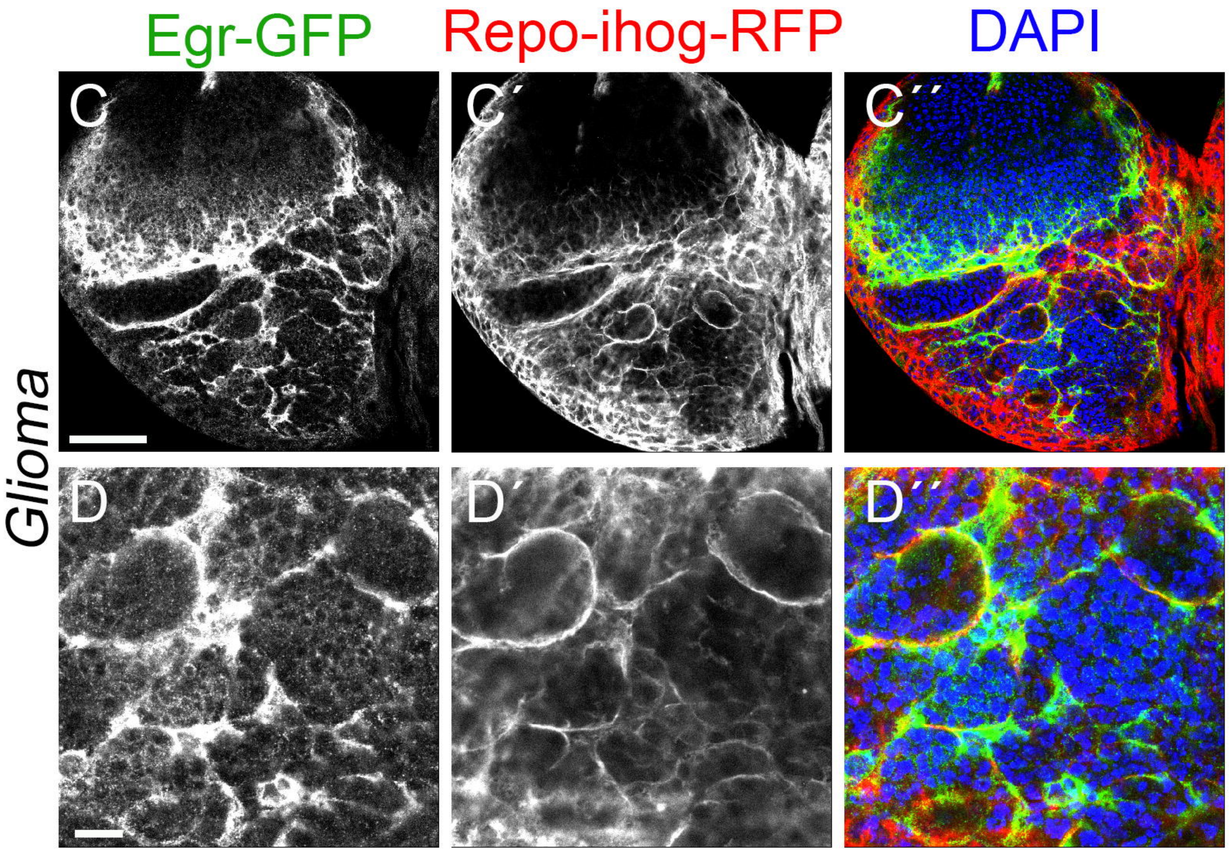

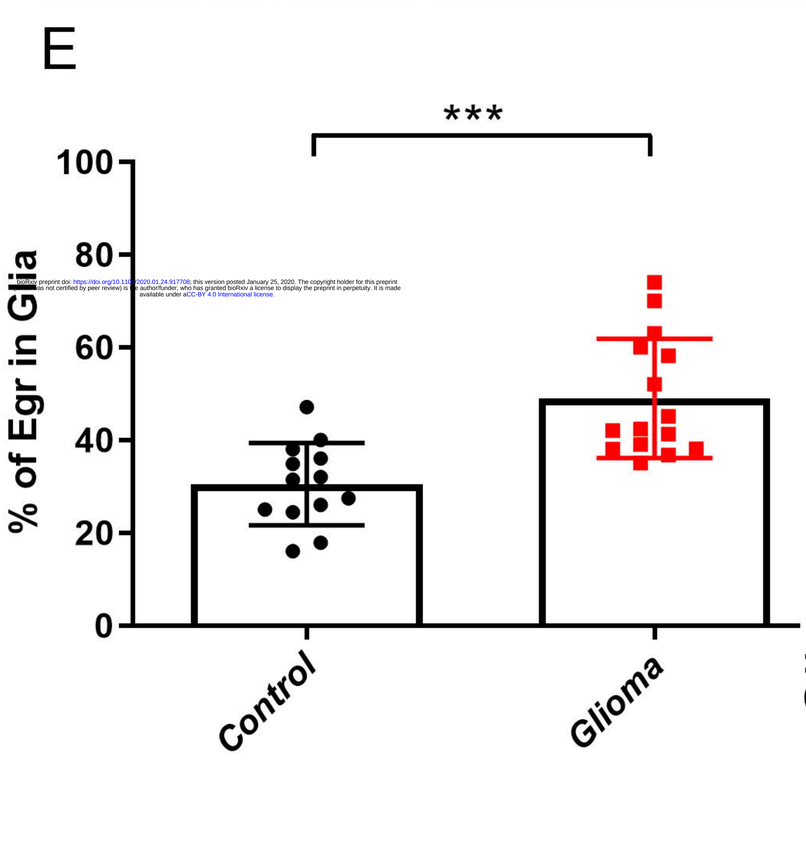

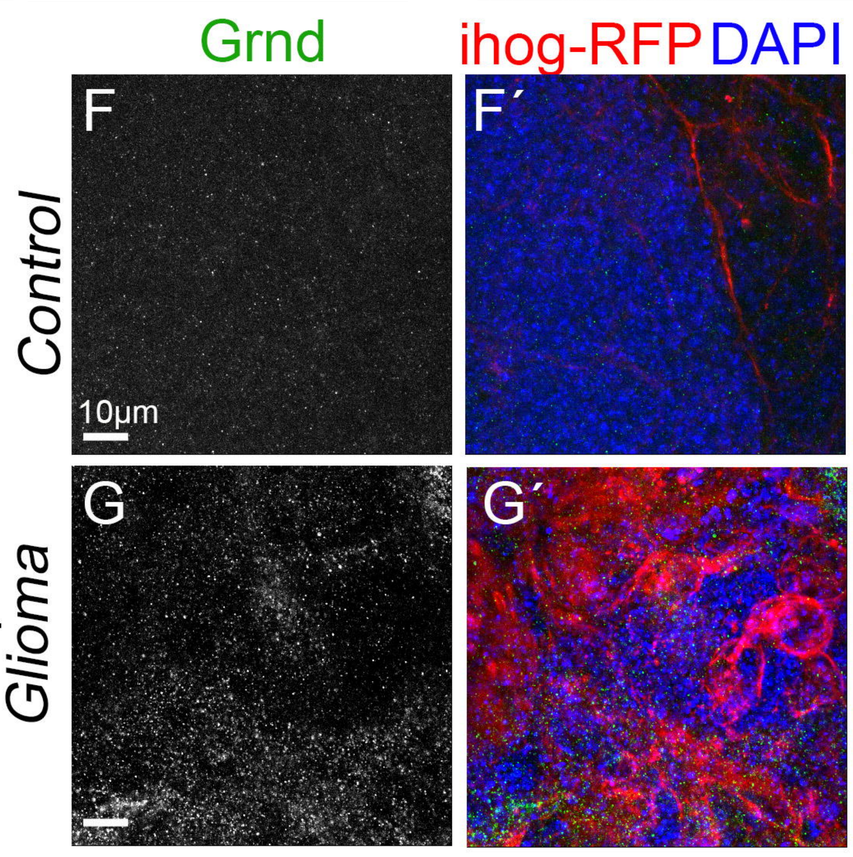

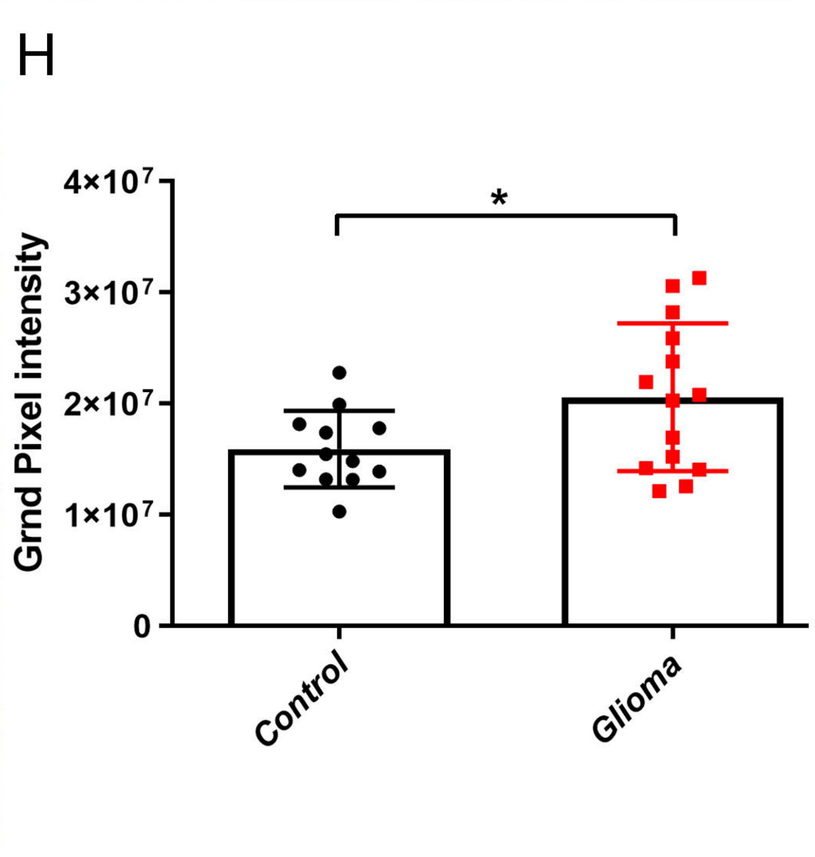

Figure 3

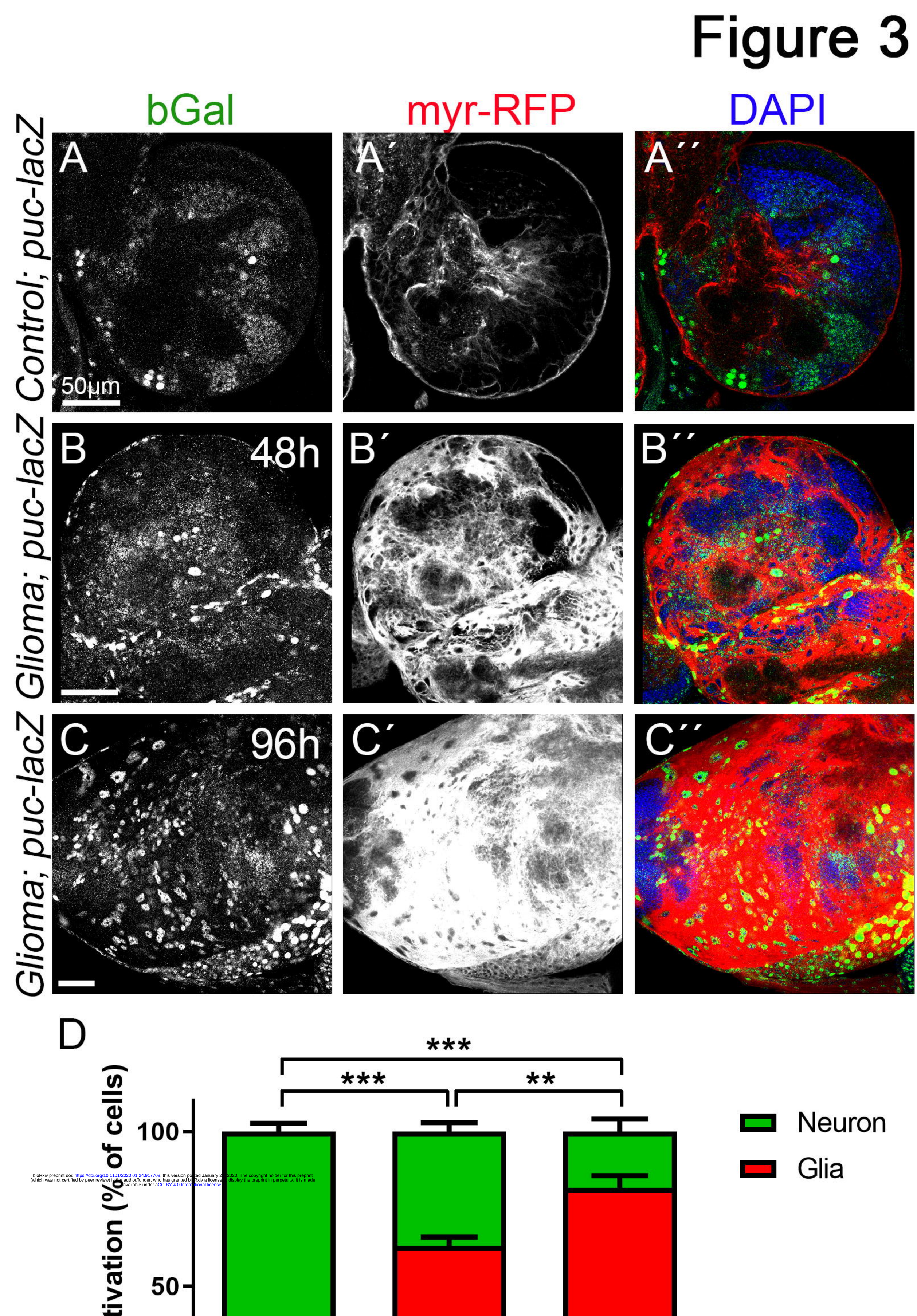

Figure 4

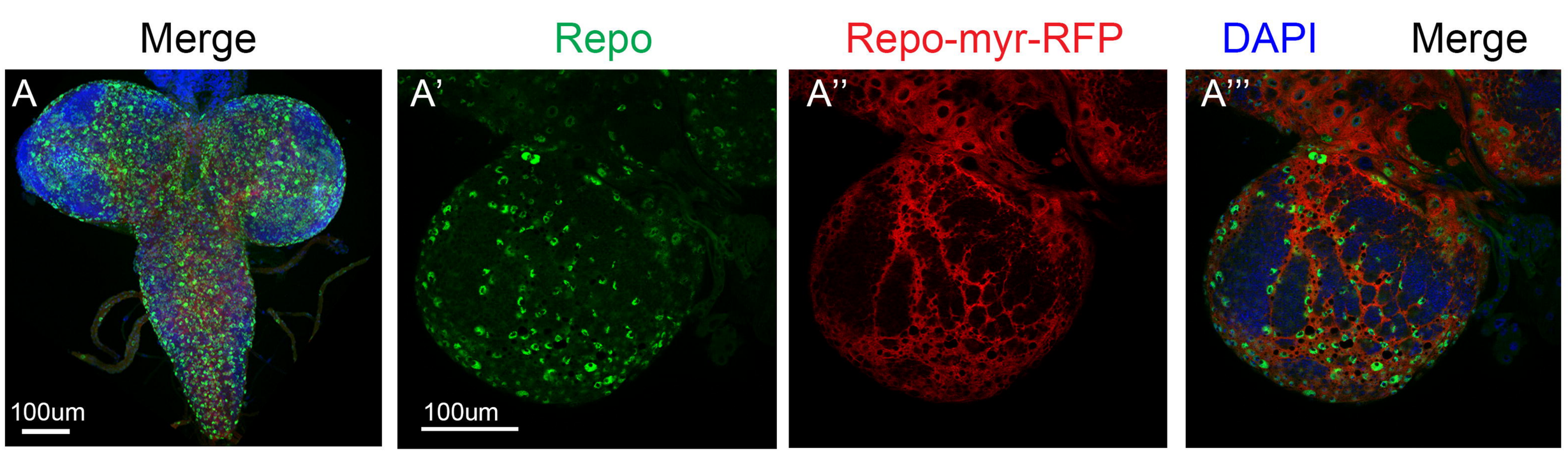

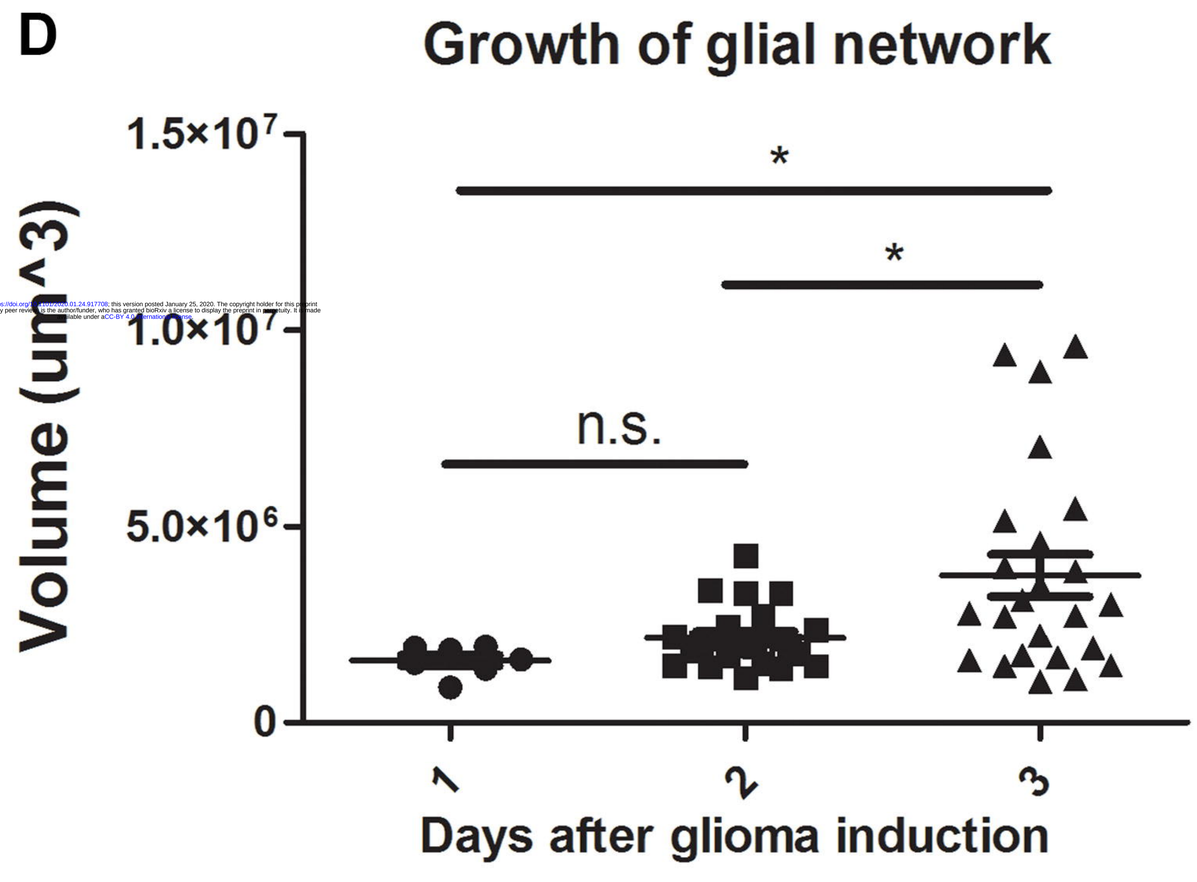

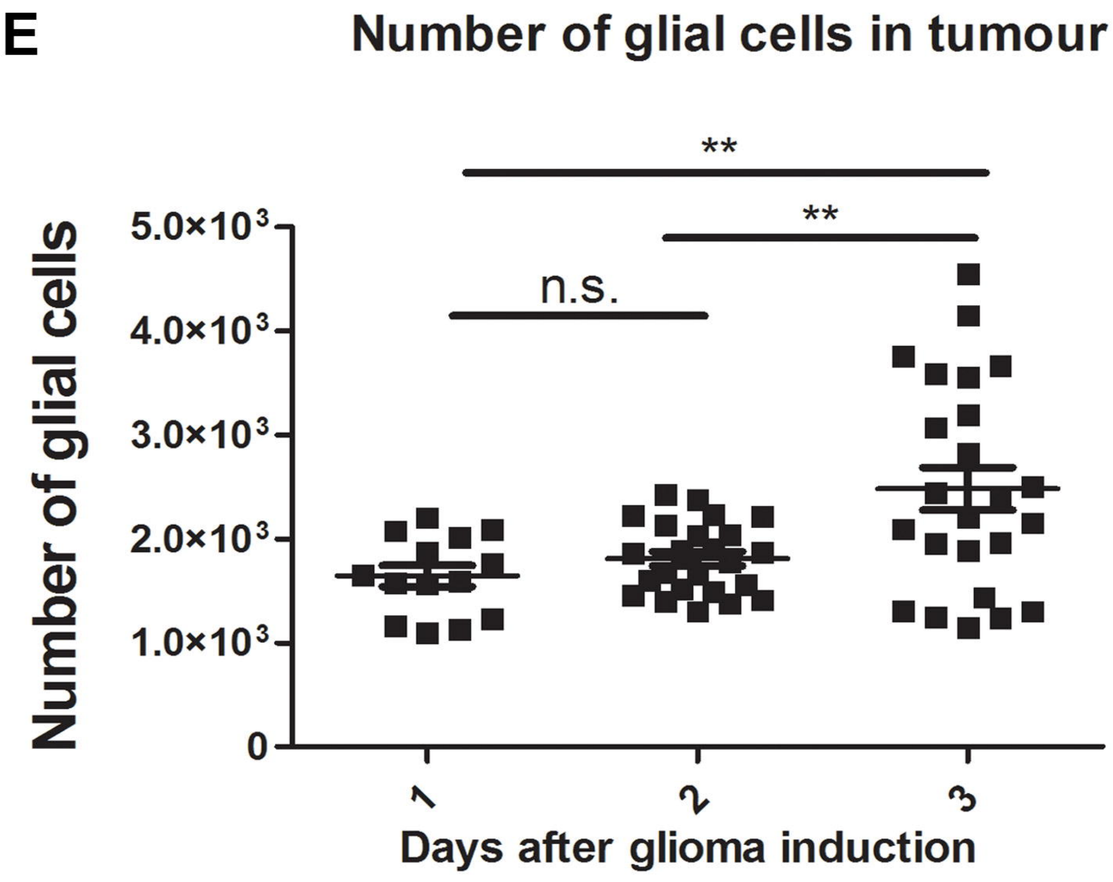

Figure 5

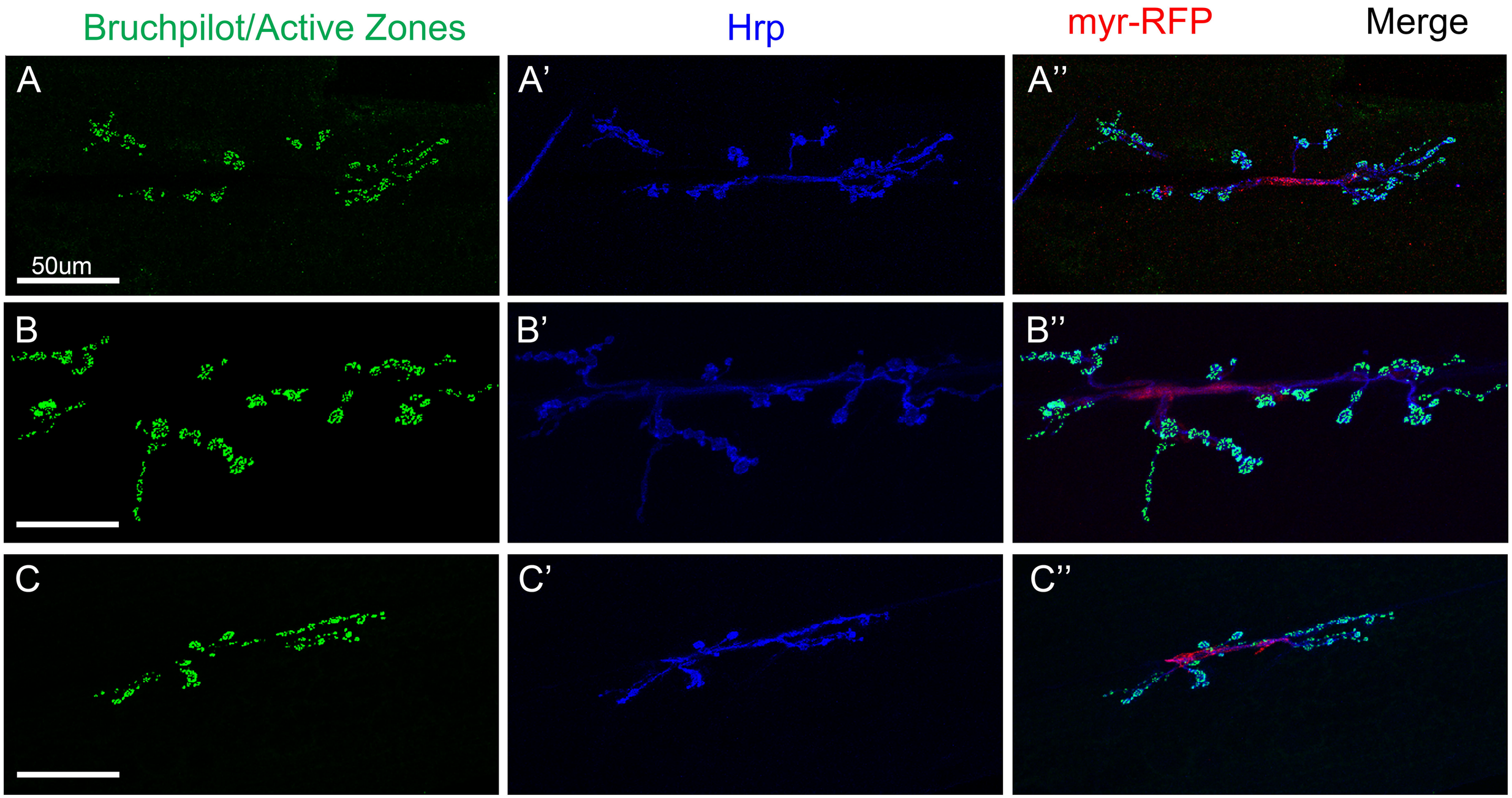
Bruchpilot/Active Zones
Hrp
myr-RFP
Merge
A
A'
A''
50um
Glioma 1D
B
B'
B''
Glioma 2D
C
C'
C''
Glioma 3D

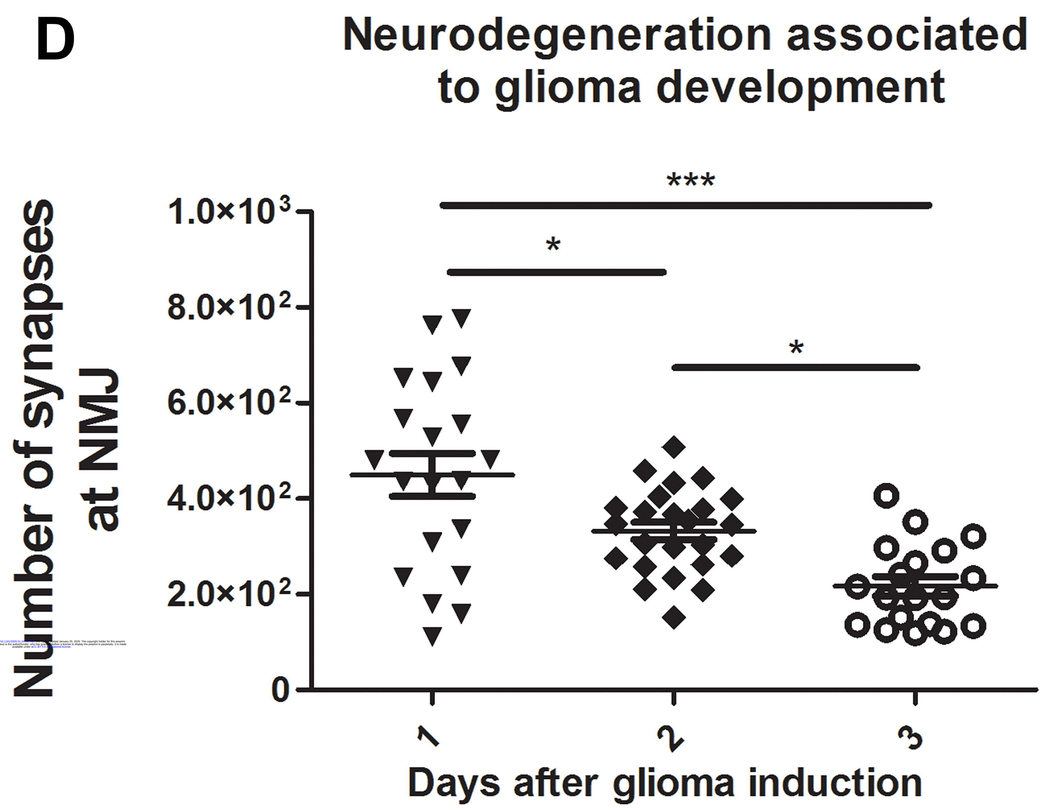
D
Neurodegeneration associated to glioma development
Number of synapses at NMJ
1.0×10³
8.0×10²
6.0×10²
4.0×10²
2.0×10²
0
***
*
*
1
2
3
Days after glioma induction

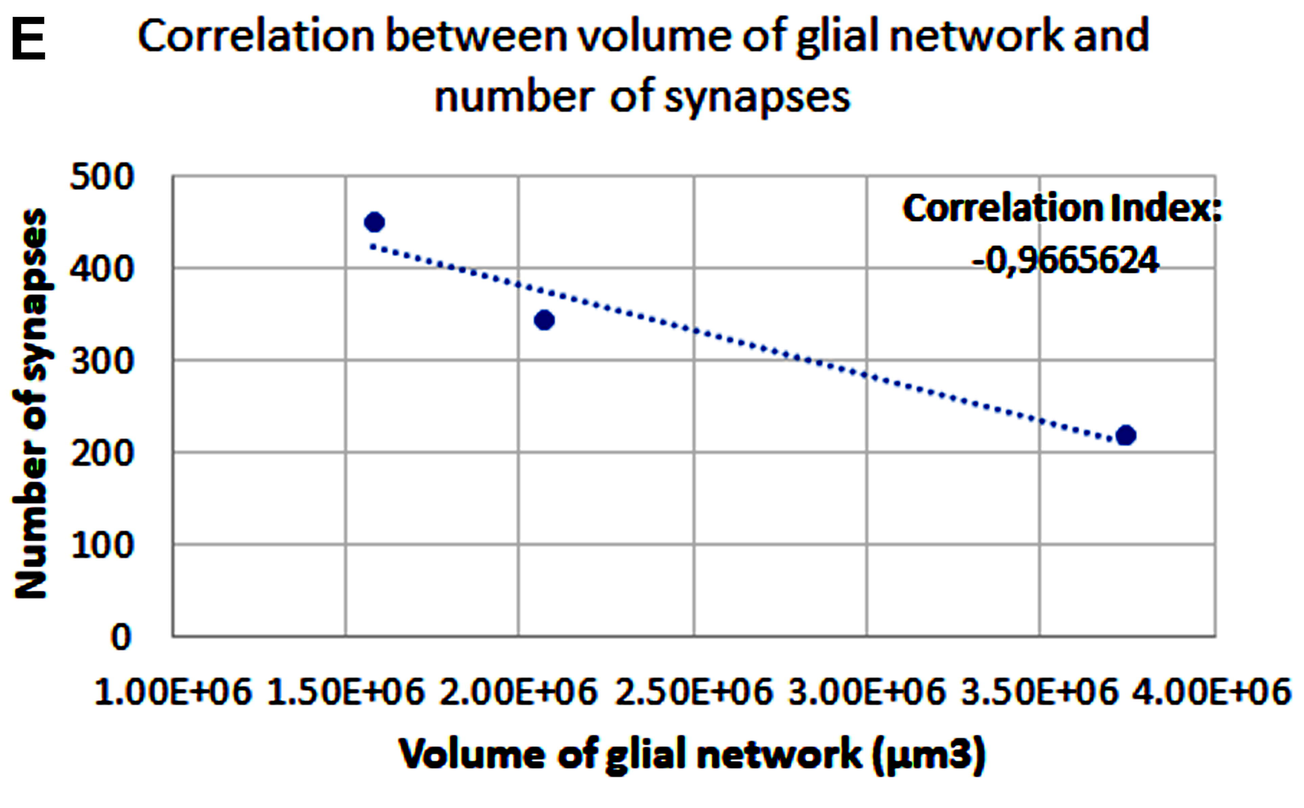
E
Correlation between volume of glial network and number of synapses
Number of synapses
500
400
300
200
100
0
Correlation Index:
-0,9665624
1.00E+06
1.50E+06
2.00E+06
2.50E+06
3.00E+06
3.50E+06
4.00E+06
Volume of glial network (µm3)

Figure S1